

## FUNCTIONS OF HEIGHT AND WIDTH DIMENSIONS IN THE INTERTIDAL MUSSEL, *MYTILUS CALIFORNIANUS*

JONATHAN N. BLYTHE<sup>1\*</sup> AND DAVID W. LEA<sup>2</sup>

<sup>1</sup>Massachusetts Institute of Technology/Woods Hole Oceanographic Institution Joint Program in Biological Oceanography, Woods Hole, Massachusetts 02543; <sup>2</sup>Department of Earth Sciences and Marine Science Institute, University of California, Santa Barbara, California 93106

**ABSTRACT** A mussel's shell records its history of growth. We investigated variability in the size and shape of mussel shells of *Mytilus californianus* Conrad (1837) to test the hypothesis that the mussel shell provides information on the contemporary condition of the mussel. Two factors were associated with shape: an epithelial discoloration and the Sr/Ca in the shell nacre. Sr/Ca data distinguished the mussel populations as did a discriminant analysis that included the trace metal ratios; Sr/Ca, Mg/Ca, Mn/Ca, Ag/Ca, Cd/Ca, Ba/Ca, and Pb/Ca. Size varied independently of shape and was not associated with the two factors. However, a null model that describes the morphological variability in height and width suggests that mussel size also plays a central role in partitioning phenotypic variability. These analyses of contemporary factors coupled with analyses of morphological variability holds promise for addressing the functional roles of mussel height and width and what proportion of phenotypic variability can be attributed to environmental factors.

**KEY WORDS:** mussel, *Mytilus californianus*, null model, shell, size, shape, epithelial discoloration, strontium, lead, morphology

### INTRODUCTION

Descriptions of mussel shell morphology help identify phenotypic variability in populations of the mussel, *Mytilus californianus* (Caceres-Martinez et al. 2003). One approach for understanding the sources of phenotypic variability is to take measurements of morphology in cross-sections of mussel populations and to associate these measurements with environmental factors that vary between populations. For example, spatial variation of height times width ( $H \times W$ ) measured from populations of *Mytilus galloprovincialis* along the coast of South Africa was associated with patterns of wave exposure (Steffani & Branch 2003). Earlier surveys of Santa Barbara *M. californianus* populations found that wave energy was related to shell area (Harger 1968) including the Campus Point population that we sample in this study.

Environmental factors such as wave exposure vary predictably at characteristic length scales, which should allow an analysis of the different sources of variability to shell morphology. At one extreme, biogeographic gradients in temperature correlate with patterns of *M. californianus* shell morphology (Dodd 1964). Point Conception has been identified as a biogeographic boundary, distinguishing *M. californianus* populations from Santa Barbara County south of Point Conception from those north of Point Conception (Blanchette et al. 2007). At the other extreme, a suite of environmental factors vary at the scale of meters over the range of elevations in the intertidal habitat. For example, *M. californianus* shell height and width varied at different locations along a mussel bed, corresponding to intertidal height (Kopp 1979).

Shell length, height, and width are measures that describe the morphology of the mussel body in three dimensions (Seed 1968). A morphometric principal components analysis (hereafter PCA) is a useful tool for addressing patterns of variability in morphological measurements (Reyment et al. 1984). What results are the first and second principal components (PC) that

relate the body size and body shape respectively (Kuris & Brody 1976). However, this technique becomes problematic when studying the relationship between size and shape, because PCs are, by definition, independent of one another. Another approach is a null model based on symmetries in the mussel body. In general, null models are not firmly grounded in biological process, and a null model of mussel height and width does not relate the biological functions of these dimensions. However, if mussel height and width dimensions meet some basic criteria of a null model, then this approach can be a useful tool for describing morphological variability.

Mussel shell morphology is a relatively slow response variable to environmental factors. More labile contemporary factors in mussels should serve as an intermediate between the source of variability in the environment and the long-term, time-integrated response apparent from morphological measurements. A red epithelial discoloration on the ventral pair of labial palps, described herein (see Fig. 2 later), is the type of variable that can change quickly enough to respond to the environmental signal occurring for example over a change in season, because epithelial tissue has the capacity to change and turn-over on shorter timescales. In contrast, the shell height and width dimensions change because of an incremental growth from shell deposition. The additional shell contributed from shell deposition can be quite small compared with the amount of shell material already accumulated by mature individuals. However, the trace metal composition of this incremental shell growth is a labile contemporary factor, and because such increments of shell addition culminate over time in the morphology of the mature adult, this is an obvious first place to look for responses to the environment to link with the long term morphological pattern. In fact, measurements of shell segments have been the basis of paleontological studies. The Sr/Ca ratio is an indicator of mussel growth, for example in the mussel *Mytilus trossulus* (Klein et al. 1996) and the clams *Saxidomus giganteus* and *Mercenaria mercenaria* (Gillikin et al. 2005). In addition, trace metals measured from mussel biogenic material

\*Corresponding author. E-mail: [jblythe@whoi.edu](mailto:jblythe@whoi.edu)

can serve to indicate pollution in the marine environment, and these measurements of pollution also have association with the height over the width (H/W) of the mussels *Mytilus edulis* (Lobel et al. 1991) and *Mytilus californianus* (Lares et al. 2005). We describe the link between these contemporary measures and mussel morphology, and based on this evidence we discuss possible functional roles of the height and width dimensions.

#### METHODS

We collected 714 mussels, *Mytilus californianus*, from a 6-cm size class from four rocky intertidal sites along the Santa Barbara coastline (Fig. 1). Thirty individuals were selected from random patches at each site for each month from November 2001 to April 2002. Error in length class selection, which was reflected in the standard deviation among the 714 length measurements (0.37 cm), was inevitable, because mussels approximating the size class were haphazardly collected within each random patch. Mussels were deposited live within two hours of collection in running sea water at the UCSB Marine Laboratory. Mussels were measured within 48 h of collection. The mussel length, the longest anterior to posterior dimension, height, the longest dorsal to ventral dimension, and width, the longest valve to valve dimension, as described by Seed (1968), were measured using dial calipers that were accurate within a hundredth of a cm. Shell dimension data were log transformed, normalized and centered on zero. A PCA was conducted on these transformed data and the first two principal components were compared with two common combinations of height and width dimensions, the height times the width ( $H \times W$ ) and the height divided by the width (H/W). Site averages and 99% confidence intervals were calculated for the PC 1, PC2,  $H \times W$ , and H/W variables for the comparison of these sites.

We derived an expression (Eqs. 1 and 2) to further analyze the morphological variability between four mussel populations. The derivation of the equation (see the appendix) groups the height and width variables into recognizable terms like the shape function,  $h/w$ , the size function,  $h \times w$ , and a difference between the height and width dimension ( $h - w$ ). The grouping of these terms results from algebraic manipulations of equations that implicitly relate the height and width dimensions.

One prerequisite of this derivation, is that the height and width dimensions must be negligibly different so that the arithmetic mean can be approximated by the geometric mean (Eq. 3). This is true when an individual's height dimension is equal to its width dimension, or nearly so. An early study on the shell dimensions in the mussel, *M. californianus*, noted that as individuals reach their maximum length, the width dimension grows with such positive allometry that it could exceed the height dimension (Coe & Fox 1942). Therefore, this assumption could be satisfied by sampling mature mussels from each site that have recently or soon will have shell growth that have intersecting trajectories of the height and width dimensions.

$$\frac{h}{w} = e^{c(h-w)} \quad (1)$$

$$c = \frac{1}{\sqrt{hw}} \quad (2)$$

$$\sqrt{hw} \cong \frac{h+w}{2} \quad (3)$$

We assessed how well the null model described the height and width of mussels collected at each site. First, we calculated

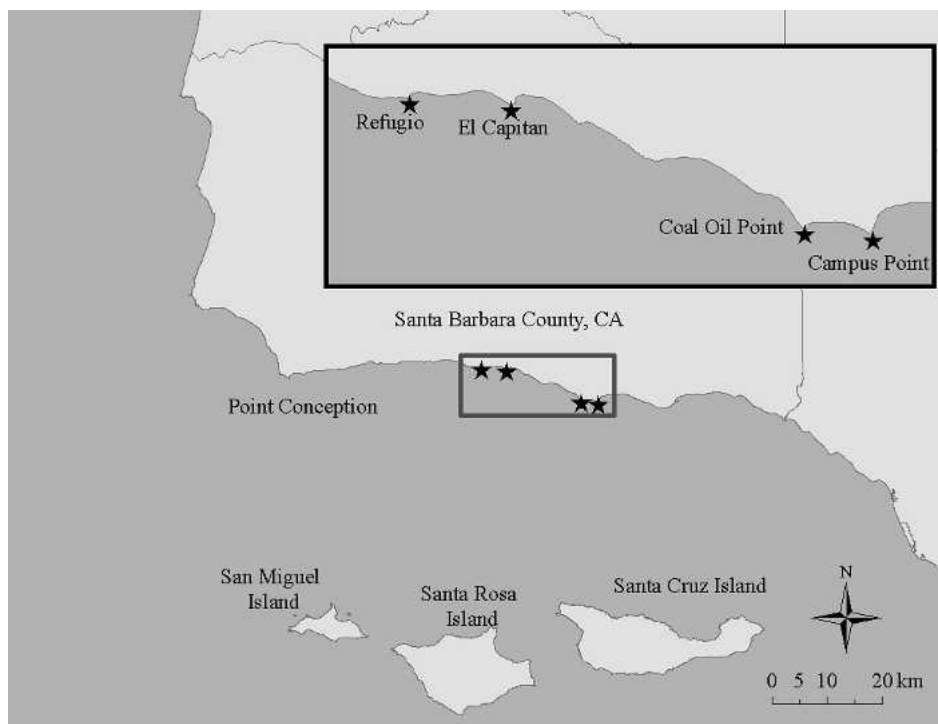


Figure 1. Four mussel populations were sampled along 20 km of the Gaviota coast in Santa Barbara County, CA.

the constant,  $c$ , by inputting the height and width measurements for each individual into Eq. 2. We calculated the site mean and 95% confidence interval for these individual mussel values of  $c$ . For comparison we also calculated the constant,  $c$ , by fitting a least squares model from Eq. 4 to data from each of the populations. The natural logarithm of the shape function was regressed against the difference between the height and the width using the *linest* function in Microsoft Excel. This relationship must pass through the origin because of the mathematical relationship between these two variables, so we set the  $y$  intercept value to pass through the origin. A 95% confidence interval was calculated for the regression parameter based on the standard error output from the *linest* function. We compared these two values of the constant,  $c$ , to test the ability of the null model to describe the morphology of mussels at each site.

$$\log\left(\frac{h}{w}\right) = c(h - w) \quad (4)$$

The ventral pair of labial palps were dissected for observation under a dissection microscope at  $\times 31$ . The labial palps were oriented in a standard position to make consistent observations among individuals. An epithelial discoloration of unknown etiology was apparent at  $\times 31$  magnification for most individuals. The discolored area was usually concentrated near the ventral margin of the palp (Fig. 2). We measured the extent of the discoloration by estimating the percentage of the surface area of the labial palp dorsal from the ventral margin that was discolored in 10% classes.

Mussel shells were prepared for chemical analysis. The shells were scraped with a stainless steel scalpel to remove the tissue, rubbed clean, dried, and then stored in plastic bags. Five shells that were between 6 and 6.5 cm in length were subsampled from those collected as described above for each of four sites for the months November 2001 to March 2002. The shells that were closest to 6 cm in length were selected for the chemical analysis. Some of the shells used in the chemical analysis were collected in a preliminary study before November 2001. There were mussel shells from El Capitan and Refugio (May 2001) and mussel shells from Campus Point and Coal Oil Point (April, May, June, July, September and October 2001, and April 2002).



Figure 2. The discoloration is readily apparent on the labial palp epithelial surface under  $\times 50$  magnification. It is concentrated at the left, near the ventral margin, and tapers off to the right.

A diamond saw was used to cut the left valve two to three cm behind the edge of elongation perpendicular to the length axis. The shell fragments containing the edge of elongation were washed together with other shells from the same group, first four times with distilled water, then four times with milliQ water, and lastly for seven hours in 40 mL of pH 7 concentrated hydrogen peroxide. The shell fragments were lined up on a pyrex dish, covered with pyrex glass, and then cooked overnight in a muffle furnace at temperatures up to 450°C according to (Bourgoin 1988, Bourgoin 1990, and Rivero & Lares 2004).

Fifty micrograms of calcium carbonate were collected from the most recently deposited material in the nacreous layer (Rivero & Lares 2004). The calcium carbonate from the four shells fragments that had been washed together were combined into one 500  $\mu$ L milliQ washed plastic vial. For the 2001 mussels, duplicates were made of the same shells by collecting another 50  $\mu$ g from each of the four shell fragments and placing the material in a second vial. The 2002 samples were replicated once with a different subset of shells. Excluding duplicates, 10 different groups of mussels were sampled from El Capitan and Refugio, 15 groups of mussels were sampled from Coal Oil Point, and 16 different groups of mussels were sampled from Campus Point. A total of 200  $\mu$ g of calcium carbonate (400  $\mu$ g with the duplicates) was collected from each set of shells.

The shell material was washed several times with milliQ water, methanol, and 0.001N HNO<sub>3</sub>, and then transferred to acid washed 500- $\mu$ L vials. The shell material was stored until the day of analysis when it was dissolved in 500  $\mu$ L of 1% HNO<sub>3</sub>. A 70-min sonication ensured complete dissolution. Molar Mg/Ca, Mn/Ca, Sr/Ca, Ag/Ca, Cd/Ca, Ba/Ca, and Pb/Ca ratios were measured by an inductively coupled plasma mass spectrometer (ICPMS) using a technique developed for analysis of fossil foraminifera (Rosenthal et al. 1999). Precision was better than  $\pm 5\%$  (1 SD) for all measurements. Accuracy was assessed by comparing measurements for two standards to known values. Measurements were accurate to  $\pm 5\%$  (1SD) except for the Cd/Ca ratio that had an accuracy of  $\pm 15\%$ .

## RESULTS

Most of the variability in length, height, and width dimension measurements was described by the first two principal components (Table 1). These two principle components were also related to two variables of height and width:  $H \times W$  and  $H/W$  (Table 2). The orthogonal principal components and the related variables of height and width were significantly different between the mussels collected at four intertidal sites (Table 3). The first principal component and  $H \times W$  variable distinguished Campus Point and Coal Oil Point from El Capitan and Refugio, but the second principal component and the  $H/W$  variable distinguished the sites El Capitan and Coal Oil Point

TABLE 1.

The loadings and percent variance explained by the first two principal components.

	Length	Height	Width	Variance
PC 1	-0.681	-0.535	-0.500	58.1%
PC 2	0.013	0.674	-0.739	30.0%

**TABLE 2.**  
Two variables correlate with the PC1 and PC2. The R statistic is reported in the table.

	H × W	H/W
PC 1	-0.904	0.025
PC 2	-0.098	1.000

from Refugio and Campus Point (Table 3). The null model also described variability in the height and width dimensions. The slope parameter,  $c$ , matched the population averages of  $c$  except at El Capitan where they were significantly different at a 95% level of confidence (Table 4). We observed that the mussel predator, *Pisaster* spp., was abundant at El Capitan, and given the important effects that predators have on *M. californianus* shape (Robles et al. 1990) and size (Paine 1976), we believe that this might be an important detail to help explain morphological variability.

The epithelial discoloration was highly variable from field to field at high magnification under a compound microscope. However, at low magnification while using a dissecting microscope, the labial palp epithelium appeared uniform enough to assess the percent cover of red debris on the whole organ (Fig. 2). Although the origin of this discoloration is unknown, it was a pronounced epithelial condition that likely indicates some physiological condition or perhaps a feeding status of an individual mussel. Populations had significantly different percent cover of discoloration in the labial palp organ (Table 5). There is much scatter about the correlation between the degree of discoloration and the shape, but a plot of the average shape of mussels in each percent discoloration category suggests that these variables have a negative association (Fig. 3).

The temporal structure of the sampling design allowed us to investigate trends in the trace metal data. The time-series of the Pb/Ca ratio starts at values around 0.3  $\mu\text{mol/mol}$  and decreases over the following months (Fig. 4). This monotonic decrease is likely a lingering effect from a heavy rain that occurred in March 2001 that is reported to have loaded terrestrial nutrients into the coastal water (McPhee-Shaw et al. 2007). We hypothesize that the terrestrial runoff mobilized trapped Pb in local watersheds, transporting Pb to near-shore waters, which was then incorporated into mussel shells. The 2002 rainy season was comparatively weaker and may have resulted in less terrigenous contribution to the trace metal signatures in mussel nacre, although the last measurements in April 2002 indicate another peak in the Pb/Ca ratio. The Sr/Ca ratio did not have any pronounced trends over the one-year time-series. The Sr/Ca ratios were often higher at Campus Point than Coal Oil Point

(Fig. 5), and the time averages of the Sr/Ca ratio allowed a comparison of these four sites (Table 5).

A linear discriminant analysis (White & Ruttenberg 2007) of the trace metal dataset that included Mg/Ca, Mn/Ca, Sr/Ca, Ag/Ca, Cd/Ca, Ba/Ca, and Pb/Ca ratios correctly placed mussels in their population for 36% of the samples ( $P = 0.056$ ). Once we discovered the apparent spike in Pb/Ca ratio during the first months of the time-series, we recomputed the discriminant analysis for data from a shorter duration between September 2001 to April 2002. The proportion of correct classifications increased to 54% ( $P < 0.001$ ), suggesting that the shorter dataset better distinguished trace metal patterns between populations. Despite this, we used the entire Sr/Ca ratio record to make a site comparisons (Table 5) because the site differences were more pronounced than the changes in the record over time.

## DISCUSSION

A variety of studies on the mussel, *Mytilus californianus*, give us some context to hypothesize functions of mussel height and width. The individual filtration rate might be associated with height among mussels of the same length class, because this dimension will determine the relative size of the filtering organ. Food availability affects the growth rate of mussels (Dahlhoff & Menge 1996). However, it is not the only factor that affects patterns of growth in the mussel, a complication that could explain the poor linear correlations with food availability in the area where this study was conducted (Phillips 2005). The shell width is hypothesized to contribute to basal metabolism for a variety of reasons. Wider mussels have more tissue that confers metabolic cost. The heat stress experienced by mussels (Helmuth 1998) is partially determined by its morphology. The width dimension would increase the rate of light absorbance, because this increases the surface area that is exposed to normally incident solar radiation. Also, an individual's energy expended in attachment to the substrate is shape dependent, because an increase in width would increase the lift that it experiences when exposed to wave action, as suggested for the congener *Mytilus galloprovincialis* (Steffani & Branch 2003). This is especially an issue for large mussels that expend more energy to remain attached (Bell & Gosline 1997). We propose the heuristic that height and width dimensions relate to positive and negative metabolic functions in individual mussels. We cannot draw on the physiological ecology literature to assess the generality of this hypothesis, because studies of this and other species of mussels have not used the height and width dimensions (Fox et al. 1937, Jones et al. 1992, Meyhofer 1985, Rao 1953, Riisgard 2001, Salkeld 1995, Sukhotin et al. 2006).

Three alternative hypotheses for the functional role of height and width dimension were considered. First, there is the

**TABLE 3.**  
Population means of PC1 and 2 and the variables of height and width with 99% CI.

	PC 1	H × W (cm <sup>2</sup> )	PC 2	H/W ratio
El Capitan ( $n = 178$ )	0.370 (0.197)	6.290 (0.160)	0.411 (0.169)	1.19 (0.03)
Coal Oil Point ( $n = 177$ )	-0.695 (0.219)	7.302 (0.197)	0.290 (0.172)	1.16 (0.03)
Refugio ( $n = 180$ )	0.316 (0.264)	6.349 (0.188)	-0.180 (0.163)	1.09 (0.03)
Campus Point ( $n = 179$ )	0.010 (0.279)	6.542 (0.188)	-0.526 (0.171)	1.04 (0.03)

TABLE 4.

The ability of the null model to describe morphological variability at each site is tested by comparing the calculated value for the coefficient, *c*, using two different techniques.

	El Capitan	Refugio	Campus Point	Coal Oil Point
Null Model <i>c</i> , (Eq. 2)	0.0401 (0.0004)	0.0400 (0.0004)	0.0394 (0.0004)	0.0373 (0.0004)
Least Squares <i>c</i> , (Eq. 4)	0.0407 (0.0003)	0.0396 (0.0004)	0.0390 (0.0004)	0.0370 (0.0004)

possibility of parasite induced morphological modification (Miura et al. 2006). Parasites, like copepods (Caceres-Martinez & Vasquez-Yeomans 1999) and turbellarians (Murina & Solonchenko 1991), were abundant in the populations that we studied (unpublished data). Second, the previously observed correlation of shell shape in toxicant bio-accumulation in *M. edulis* (Lobel et al. 1991) suggests a functional role. We detected seasonal peaks in Pb/Ca, however, these levels were well below those measurements from *M. edulis* collected in polluted habitats (Bourgoin 1990). Third, predation may have a variety of effects on mussel shape. The classical hypothesis is that large mussels escape predation because of a size refuge (Paine 1976). *Pisaster* spp. predation is not an important source of predation south of Point Conception (Menge et al. 2004), although we observed high densities of *Pisaster* spp. at El Capitan suggesting that predation was prevalent there. Mussels at El Capitan have high H/W measures that are characteristic of quickly growing mussels (Coe & Fox 1942), an observation that supports the inference of a size refuge effect. Lobsters are also predators of mussels, and their predation affects mussel morphology in particular ways that are not completely captured by the length, width, and height dimensions that we analyze here (Robles et al. 1990). However, increased shell thickness from induced defense (Leonard et al. 1999) may contribute to the width dimension of mussel shells.

We analyzed the morphology of mussels to address the hypothesized functional roles of mussel height and width. The  $H \times W$  variable is highly correlated with the first principal component indicating its relationship to mussel size. However,  $H \times W$  does not correspond to any physically intuitive property of mussels, like the cross sectional area of mussels, because the dimensions of height and width are not necessarily measured in the same plane. The convention is to measure the maximum height and the maximum width that often occur at different lengths along the mussel's axis. The coefficient, *c*, in the null model has a more intuitive relationship to mussel size, because it is a scaling factor for the absolute differences between

the height and width of mussel shells. Another way to think of these height and width dimensions is that the square root of the product is an average diameter.

The null model gives a good description of morphological variability within each of the sites, which is a surprising result given the range of environmental conditions that mussels may experience in different locations, either on the high or the low tide or the exposed or protected portions within each site. An assumption of the null model is the linearization about the point where the height dimension equals the width dimension. The height and width dimensions intersect in their growth trajectories (Coe & Fox 1942, Seed 1968), and the assumption of the linearization can be strengthened by collection of mussels from the length class where many of the individuals in a population have recently or will soon experience the intersection of the height and width growth trajectories. Six-centimeter mussels were collected from four populations. These mussels do not represent the entire population at these sites, but they do represent all of the possible locations that mussels could live, because mussel beds were sampled at random. Although it was useful to collect mussels from a length class for the purposes of reducing the number anatomical dimension necessary for our null model morphological analysis, only the Refugio and Campus Point sites met the null model assumption of nearly equal height and width dimensions necessary to satisfy Eq. 3. El Capitan and Coal Oil Point mussels had fewer individuals with nearly identical height and width dimensions. We suspect that the null model is relatively robust in this respect, but we cannot rule out whether this accounts for the disagreement between the null model calculation of *c* and the least squares estimate of *c* for El Capitan mussels (Table 4).

Measurements of the discoloration of the labial palp tissue and trace metals in the nacre distinguish the mussel populations. We noticed that the labial palp discoloration related to the H/W variable and varied consistently between mussel populations in

TABLE 5.

Means of contemporary factors, with 99% CI and sample size in parentheses.

	Percent Cover of Labial Palp Red Discoloration	Sr/Ca (mmol/mol)
El Capitan	11 (3, <i>n</i> = 178)	1.736 (0.081, <i>n</i> = 14)
Coal Oil Point	13 (3, <i>n</i> = 177)	1.750 (0.079, <i>n</i> = 24)
Refugio	38 (5, <i>n</i> = 180)	1.900 (0.118, <i>n</i> = 14)
Campus Point	40 (6, <i>n</i> = 179)	1.941 (0.120, <i>n</i> = 26)

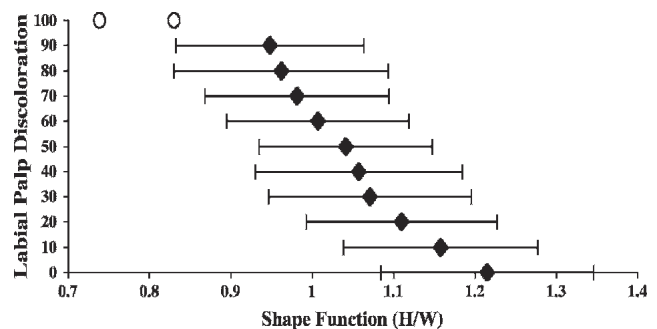
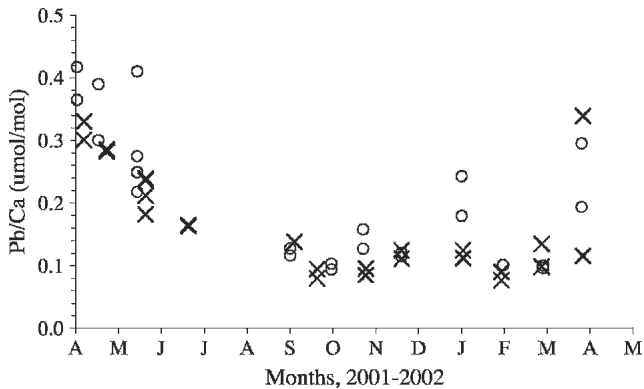


Figure 3. The shape of mussels was averaged (diamonds) for each category of discoloration and is plotted with the standard deviation of the shape (error bars). Two circles are outlier individuals.



**Figure 4.** Pb/Ca ratio data collected at Campus Point (x marks) and Coal Oil Point (circles) from 4/2001 through 4/2002. Each site and date has two to four values representing replicate aragonite samples collected from the same or similar mussels.

a preliminary study (data not reported), so this new measurement was collected on every individual in this study to better document that pattern. A variety of epithelial measurements have been described for *M. californianus*, relating the cellular response to various stimuli (Bayne et al. 1979, Thompson et al. 1978) and an immunological response to toxicants (Luenger et al. 2004). Assays that focus on the epithelium have been developed for other species, including a scallop (MacDonald et al. 1995), and a Baltic Sea mussel (Smolarz et al. 2006). Whereas it is clear from our investigations that the labial palp discoloration is a labile and contemporary measure that significantly distinguishes these populations in a way consistent with the shell shape measurement, it is unclear whether the epithelial discoloration is a condition that is consequential to the morphology of mussels. We hypothesize that the shell shape modulates the physiological functions of mussels, which are then proximately apparent in the measures of epithelial discoloration.

Geochemical studies have demonstrated that the Sr/Ca ratio in the bivalve shell reflects the biochemical composition of anatomical regions where the shell is formed (Klein et al. 1996). Often, the relation of Sr/Ca to physiology is species specific, making it difficult to generalize these findings to the mussel *Mytilus californianus*. An early study found a negative trend of percent molar Sr with temperature in *Mytilus* spp. aragonite

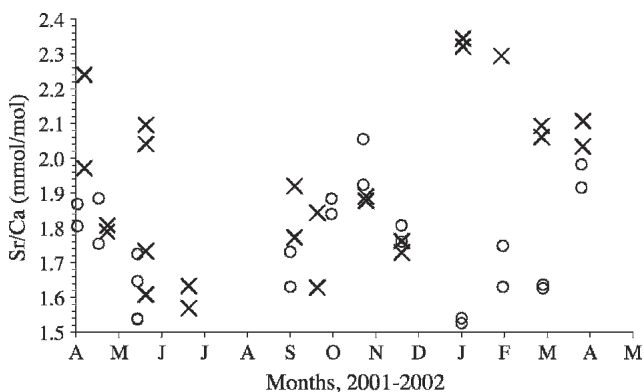


**Figure 5.** Sr/Ca ratio data collected at Campus Point (x marks) and Coal Oil Point (circles) from 4/2001 through 4/2002. Each site and date has two to four values representing replicate aragonite samples collected from the same or similar mussels.

(Dodd 1965), but we cannot confirm such a trend with our data. This species may have been overlooked for continued paleontological research because of the difficulty of ageing individuals using growth bands (Richards 1928). The only published technique relies on differential growth of the aragonite and inner calcite layers that form seasonal toothed patterns in the shell cross sections (Dodd 1964). This method is not applicable to all individuals, because the inner calcite layer does not form in some fast growing individuals and is mostly absent in some Santa Barbara populations (unpublished data).

Other generalities can be drawn from the geochemical literature to help interpret the Sr/Ca ratio results. Age may be a confounding factor in these analyses, because 6-cm mussels from different populations may have different ages. Patterns of the Sr/Ca ratio in fossil bivalve shells are relatively more difficult to resolve in mature portions of the shell relative to the juvenile portions because of the dramatic decrease in shell deposition that bivalves experience on reaching maturity (Freitas et al. 2005, Purton et al. 1999). Lobel et al. (1991) observed associations between the H/W variable and Sr measured from mantle tissue. They described the H/W variable as an indication of "physiological age." Presumably, this concept relates more to metabolic function of an individual rather than its actual chronological age, but it is difficult to know, because age and physiological condition are auto-correlated. Therefore, it is often beneficial to examine more proximal causes of Sr/Ca variability (Gillikin et al. 2005).

We hypothesize that the labial palp epithelial tissue discoloration and Sr/Ca ratio are contemporary measures of mussel physiology that indicate physiological variability between mussels from these four sites. Although mantle tissue is involved in the calcification process that ultimately controls the Sr/Ca ratio in the mussel shell, the discoloration that we measured occurs on the labial palp, a feeding organ that is not directly involved in calcification. Not only do these contemporary measures agree in how the site variability is partitioned, the shape variables (PC2, H/W) distinguish the mussels from these sites in the same manner. All three variables distinguish El Capitan and Coal Oil Point from Refugio and Campus Point, which supports the conclusion of physiological differences between these populations. The size variable, on the other hand, places the populations in a different order and instead distinguished El Capitan and Refugio from Campus Point and Coal Oil Point. Size and shape provide different information on the phenotypic variability between mussel populations.

In the future, we would suggest selecting a length class that is specific for each site, giving the highest overall overlap with the height and width intersection. Because the value of  $c$  relates to the size of the mussel, it is apparent that selecting different length classes would likely predispose us to measure site differences in the value of  $c$ . An improved formulation of the null model would include the length dimension or somehow correct for different length classes of mussels. As is demonstrated here, a null model approach has the ability to describe a great deal of the morphological variability within a site. One of the most promising avenues for future work involves more extensive comparison of distinct mussel populations. There are few biological records that span long enough timescales to address the effect of anthropogenically induced environmental change like from global warming, or that span long enough spatial scales to address inherent scales of population variability

induced from environmental gradients. However, there is a veritable treasure trove of historical or paleontological mussel shell collections and archived datasets where these three dimensions were recorded that could be used to address these pressing ecological questions.

#### ACKNOWLEDGMENTS

A. Kuris inspired the authors to study mussel allometry and provided valuable critiques throughout the data collection, analysis, and writing phases of this research. The authors

thank R. Schmitt for discussion on pooling shells for trace metal analyses; G. Paradis for analyzing dissolved shell material by ICP-MS; S. A. Blythe for field assistance; and S. W. Blythe, H. Marsella, M. Holcomb, and an anonymous reviewer for comments on the manuscript. The authors acknowledge the UC Natural Reserve System for the mussels collected from Coal Oil Point. ICP-MS measurements were paid for by UCSB's Shoreline Preservation Fund. A University of California Undergraduate Genesis award provided funds for field equipment. Field and laboratory research was conducted by J. N. B. while attending UCSB as an undergraduate.

#### LITERATURE CITED

- Bayne, C. J., M. N. Moore, T. H. Carefoot & R. J. Thompson. 1979. Hemolymph functions of *Mytilus californianus*: the cytochemistry of hemocytes and their responses to foreign implants and hemolymph factors in phagocytosis. *J. Invertebr. Pathol.* 34:1–20.
- Bell, E. C. & J. M. Gosline. 1997. Strategies for life in flow: tenacity, morphometry, and probability of dislodgement of two *Mytilus* species. *Mar. Ecol. Prog. Ser.* 159:197–208.
- Blanchette, C., B. S. T. Helmuth & S. Gaines. 2007. Spatial patterns of growth in the mussel, *Mytilus californianus*, across a major oceanographic and biogeographic boundary at Point Conception, California, USA. *J. Exp. Mar. Biol. Ecol.* 340:126–148.
- Bourgoin, B. P. 1988. A rapid and inexpensive technique to separate the calcite and nacreous layers in *Mytilus edulis* shells. *Mar. Environ. Res.* 25:125–129.
- Bourgoin, B. P. 1990. *Mytilus edulis* shell as a bioindicator of lead pollution: considerations on bioavailability and variability. *Mar. Ecol. Prog. Ser.* 61:253–262.
- Caceres-Martinez, J., M. A. Rio-Portilla, S.C.-R. Gutierrez & I. M. G. Humaran. 2003. Phenotypes of the California mussel, *Mytilus californianus*, Conrad (1837). *J. Shellfish Res.* 22:135–140.
- Caceres-Martinez, J. & R. Vasquez-Yeomans. 1999. Metazoan parasites and pearls in coexisting mussel species: *Mytilus californianus*, *Mytilus galloprovincialis*, and *Septifer bifurcatus*, from an exposed rocky shore in Baja California, Northwest Mexico. *Veliger* 42:10–16.
- Coe, W. R. & D. L. Fox. 1942. Biology of the California sea-mussel. *J. Exp. Zool.* 90:1–30.
- Dahlhoff, E. P. & B. A. Menge. 1996. Influence of phytoplankton concentration and wave exposure on the ecophysiology of *Mytilus californianus*. *Mar. Ecol. Prog. Ser.* 144:97–107.
- Dodd, J. R. 1964. Environmentally controlled variation in the shell structure of a pelecypod species. *J. Paleontol.* 38:1064–1071.
- Dodd, J. R. 1965. Environmental control of strontium and magnesium in *Mytilus*\*. *Geochim. Cosmochim. Acta* 29:385–398.
- Fox, D. L., H. V. Sverdrup & J. P. Cunningham. 1937. The rate of water propulsion by the Californian mussel. *Biol. Bull.* 72:417–422.
- Freitas, P., L. J. Clarke, H. Kennedy & C. Richardson. 2005. Mg/Ca, Sr/Ca, and stable-isotope (d18O and d13C) ratio profiles from the fan mussel *Pinna nobilis*: Seasonal records and temperature relationships. *Geochem. Geophys. Geosys.* Q 04D14, doi: 10.1029/2004GC000872.
- Gillikin, D. P., A. Lorrain, J. Navez, J. W. Taylor, L. Andre, E. Keppens, W. Baeyens & F. Dehairs. 2005. Strong biological controls on Sr/Ca ratios in aragonitic marine bivalve shells. *Geochem. Geophys. Geosys.* Q 05009, doi: 10.1029/2004GC000874.
- Harger, J. R. E. 1968. The effect of wave impact on some aspects of the biology of sea mussels. *Veliger* 12:401–414.
- Helmuth, B. S. T. 1998. Intertidal mussel microclimates: prediction the body temperature of a sessile invertebrate. *Ecol. Monogr.* 68: 51–74.
- Jones, H. D., O. G. Richards & T. A. Southern. 1992. Gill dimensions, water pumping rate and body size in the mussel *Mytilus edulis* L. *J. Exp. Mar. Biol. Ecol.* 155:213–237.
- Klein, R. T., K. C. Lohmann & C. W. Thayer. 1996. Sr/Ca and 13C/12C ratios in skeletal calcite of *Mytilus trossulus*: covariation with metabolic rate, salinity, and carbon isotopic composition of seawater. *Geochim. Cosmochim. Acta* 60:4207–4221.
- Kopp, J. C. 1979. Growth and the intertidal gradient in the sea mussel *Mytilus californianus* Conrad, 1837. *Veliger* 22:51–56.
- Kuris, A. M. & M. S. Brody. 1976. Use of principal components analysis to describe the snail shell resource for hermit crabs. *J. Exp. Mar. Biol. Ecol.* 22:69–77.
- Lares, M. L., L. E. Rivero & M. A. Huerta-Diaz. 2005. Cd concentration in the soft tissue vs. the nacreous layer of *Mytilus californianus*. *Mar. Pollut. Bull.* 50:1373–1381.
- Leonard, G. H., M. D. Bertness & P. O. Yund. 1999. Crab predation, waterborne cues, and inducible defenses in the Blue Mussel, *Mytilus edulis*. *Ecology* 80:1–14.
- Lobel, P. B., C. D. Bajdik, S. P. Belkhome, S. E. Jackson & H. P. Longerich. 1991. Improved protocol for collecting mussel watch specimens taking into account sex, size, condition, shell shape, and chronological age. *Arch. Environ. Contam. Toxicol.* 21:409–414.
- Luenger, A. C., C. S. Friedman, P. T. Raimondi & A. R. Flegel. 2004. Evaluation of mussel immune responses as indicators of contamination in San Francisco Bay. *Mar. Environ. Res.* 57:197–212.
- MacDonald, B. A., J. E. Ward & C. H. McKenzie. 1995. Exfoliation of epithelial cells from the pallial organs of the sea scallop, *Placopecten magellanicus*. *J. Exp. Mar. Biol. Ecol.* 191:151–165.
- McPhee-Shaw, E., D. A. Siegel, L. Washburn, M. Brzezinski, J. L. Jones, A. Leydecker & J. Melack. 2007. Mechanisms for nutrient delivery to the inner shelf: Observations from the Santa Barbara Channel. *Limnol. Oceanogr.* 52:1748–1766.
- Menge, B. A., C. Blanchette, P. T. Raimondi, T. Freidenburg, S. Gaines, J. Lubchenco, D. Lohse, G. Hudson, M. Foley & J. Pamplin. 2004. Species interaction strength: testing model predictions along an upwelling gradient. *Ecol. Monogr.* 74:663–684.
- Meyhofer, E. 1985. Comparative pumping rates in suspension-feeding bivalves. *Mar. Biol.* 85:137–142.
- Miura, O., A. M. Kuris, M. Torching, H. Rauthor & C. Sauthor. 2006. Parasites alter host phenotype and may create a new ecological niche for snail hosts. *Proc. Royal Society B* 273:1323–1328.
- Murina, G. V. & A. I. Solonchenko. 1991. Commensals of *Mytilus galloprovincialis* in the Black Sea: *Urostoma cyprinae* (Turbellaria) and *Polydora ciliata* (Polychaeta). *Hydrobiologia* 227: 385–387.
- Paine, R. T. 1976. Size-limited predation: an observational and experimental approach with *Mytilus-Pisaster* interaction. *Ecology* 57:858–873.
- Phillips, N. E. 2005. Growth of filter-feeding benthic invertebrates from a region with variable upwelling intensity. *Mar. Ecol. Prog. Ser.* 295:79–89.

Purton, L. M. A., G. A. Shields, M. D. Brasier & G. W. Grime. 1999. Metabolism controls Sr/Ca ratios in fossil aragonitic mollusks. *Geology* 27:1083–1086.

Rao, K. P. 1953. Rate of water propulsion in *Mytilus californianus* as a function of latitude. *Biol. Bull.* 104:171–181.

Reyment, R. A., R. E. Blackith & N. A. Campbell. 1984. Multivariate Morphometrics. London, Academic Press Inc.

Richards, O. W. 1928. The growth of the mussel *Mytilus californianus*. *Nautilus* 41:99–101.

Riisgard, H. U. 2001. On measurement of filtration rates in bivalves- the stony road to reliable data: review and interpretation. *Mar. Ecol. Prog. Ser.* 211:275–291.

Rivero, L. E. & M. L. Lares. 2004. A technique for the separation of the most recently deposited nacreous layer in *Mytilus californianus* shells for trace metal analysis. *Ciencias Marinas* 30:343–347.

Robles, C. D., D. Sweetnam & J. Eminike. 1990. Lobster predation on mussels: shore-level differences in prey vulnerability and predator preference. *Ecology* 71:1564–1577.

Rosenthal, Y., M. P. Field & R. M. Sherrell. 1999. Precise determination of Element/Calcium ratios in calcareous samples using sector field inductively coupled plasma mass spectrometry. *Anal. Chem.* 71:3248–3253.

Salkeld, P. N. 1995. Aspects of reproduction associated with the use of a segmented regression to describe the relationship between body weight and shell length of *Mytilus edulis*. *Mar. Ecol. Prog. Ser.* 124:117–128.

Seed, R. 1968. Factors influencing shell shape in the mussel *Mytilus edulis*. *J. Marine Biol. Assoc. U.K.* 48:561–584.

Smolarz, K., M. Wolowicz & M. Stachnik. 2006. First record of the occurrence of “gill disease” in *Mytilus edulis trossulus* from the Gulf of Gdansk (Baltic Sea, Poland). *J. Invertebr. Pathol.* 93:207–209.

Steffani, C. N. & G. M. Branch. 2003. Growth rate, condition, and shell shape of *Mytilus galloprovincialis*: responses to wave exposure. *Mar. Ecol. Prog. Ser.* 246:197–209.

Sukhotin, A. A., D. Abele & H.-O. Portner. 2006. Ageing and metabolism of *Mytilus edulis*: populations from various climate regimes. *J. Shellfish Res.* 25:893–899.

Thompson, R. J., C. J. Bayne, M. N. Moore & T. H. Carefoot. 1978. Haemolymph volume, changes in the biochemical composition of the blood, and cytological responses of the digestive cells in *Mytilus californianus* Conrad, induced by nutritional, thermal, and exposure stress. *J. Comp. Physiol.* 127:287–298.

White, J. W. & B. I. Ruttenberg. 2007. Discriminant function analysis in marine ecology: some oversights and their solutions. *Mar. Ecol. Prog. Ser.* 329:301–305.

$$0 = h^2 - dh - g, \quad h = \frac{d + \sqrt{d^2 + 4g}}{2} \quad (\text{A1})$$

$$0 = w^2 + dw - g, \quad w = \frac{-d + \sqrt{d^2 + 4g}}{2} \quad (\text{A2})$$

$$\frac{h}{w} = \frac{d + \sqrt{d^2 + 4g}}{-d + \sqrt{d^2 + 4g}} \quad (\text{A3})$$

$$\frac{h}{w} = \frac{4g + 2d\sqrt{d^2 + 4g} + 2d^2}{4g} \quad (\text{A4})$$

$$\frac{h}{w} = 1 + \frac{d\sqrt{d^2 + 4g}}{2g} + \frac{d^2}{2g} \quad (\text{A5})$$

$$\frac{h}{w} = 1 + \frac{d\sqrt{(h-w)^2 + 4hw}}{2g} + \frac{d^2}{2g} \quad (\text{A6})$$

$$\frac{h}{w} = 1 + \frac{d(h+w)}{2g} + \frac{d^2}{2g} \quad (\text{A7})$$

Assuming that  $h + w \cong 2\sqrt{hw}$

$$\frac{h}{w} = 1 + \frac{d}{\sqrt{g}} + \frac{d^2}{2g} \quad (\text{A8})$$

$$e^{d/\sqrt{g}} = e^{d_i} \left( 1 + \left( \frac{d}{\sqrt{g}} + d_i \right) + \frac{1}{2} \left( \frac{d}{\sqrt{g}} + d_i \right)^2 \right) \quad (\text{A9})$$

Where  $d_i$  is the difference about the intercept of  $h$  and  $w$ .  $h \cong w$  and  $d_i \cong 0$ .

$$e^{d/\sqrt{g}} = 1 + \frac{d}{\sqrt{g}} + \frac{d^2}{2g} \quad (\text{A10})$$

$$\frac{h}{w} = e^{d/\sqrt{g}} \quad (\text{A11})$$

#### APPENDIX—DERIVATION OF THE NULL MODEL

Given that  $g = hw$  and  $d = h - w$